

# The relation between the magnetic field strength and the coronal temperature of cool stars

J.R. Shi<sup>1,2</sup>, G. Zhao<sup>1</sup>, Yong-Heng Zhao<sup>1</sup>, and Jun-han You<sup>2</sup>

<sup>1</sup> Beijing Astronomical Observatory, Chinese Academy of Sciences, Beijing 100012, P.R. China

<sup>2</sup> Institute for Space Astrophysics, Department of Applied Physics, Shanghai Jiao Tong University, Shanghai 200030, P.R. China

Received 19 November 1997 / Accepted 17 August 1998

**Abstract.** The correlation between the coronal X-ray temperature and the magnetic field strength in late-type stars is investigated, based on data primarily from the ROSAT PSPC. According to the observation, we divide the stars into three groups: single, binary and RS CVn stars. From the sample of single stars, we find a clear correlation of the coronal temperature with the magnetic field strength. We interpret that result as the magnetic heating process.

**Key words:** stars: activity – stars: coronae – stars: late-type – stars: magnetic fields – X-rays: stars

## 1. Introduction

All activity at the surface of cool stars is almost certainly due to magnetic fields: the magnetic field plays a key role in our understanding of this activity and the coronal X-ray emission. These fields are required first to confine the hot X-ray emitting coronal gas, and second, they are also believed to be relevant for the coronal heating process heating the coronal plasma to X-ray emitting temperatures (Schmitt 1994).

The Yohkoh coronal X-ray images plainly show that the brightness of the corona, and hence the strength of coronal heating, is generally much stronger in the region of the strong magnetic field (active regions). This simple observation alone implies that coronal heating is a magnetic phenomenon. In terms of practical observations, we might expect the bright coronal substructures in active regions to be rooted in places that stand out in some way in photospheric magnetograms. If so, the magnetic field at these sites might shed light on the coronal heating process (Falconer et al. 1997).

Coronal heating is widespread among cool main-sequence stars, and this heating depends ultimately on mechanical energy associated with convective flows. There are two principal ways by which convection can generate mechanical energy. One is direct, in the form of acoustic waves that inevitably occur when compressible material is forced into motion. The second is indirect and relies on operation of a dynamo to give rise to magnetic fields. Mullan and Fleming (1996) suggested that the quiet

coronal regions may be heated acoustically, but that the active coronal regions are heated magnetically.

We use the Raymond-Smith model to fit the soft X-ray spectrum, and find a remarkable correlation of the coronal temperatures with the photospheric magnetic field strength for single stars, which suggest that the corona is heated magnetically. Thus we can estimate the magnetic field strength from the X-ray spectrum.

In Sect. 2 we discuss the data used in our analysis and in particular discuss the criteria used to determine the properties of the program stars. Sect. 3 contains our basic results; a comparison between the coronal temperatures and magnetic field strength is specifically presented, statistical evidence for sample stars is also presented, and finally the correlation between the coronal temperatures and the magnetic field strength is discussed. In the last section, the main conclusions are summarized.

## 2. Program stars and data analysis

### 2.1. Program stars

Our sample consists of single, binary and RS CVn stars with spectral type F-M, for which both the magnetic field strengths and ROSAT PSPC observations are available. We present the list of investigated stars in Table 1, columns (1) and (2) give sequence number and star name. The spectral type, B-V colour and adopted distance are given in columns (3), (4) and (5). Columns (6) and (7) give the magnetic field strength and the fill factor. In column (9), the S, B and R represent single, binary and RS CVn stars respectively.

### 2.2. Data analysis

We use the data of the Roentgensatellite (ROSAT) with the position sensitive proportional counter (PSPC) to obtain pointed X-ray observations of selected program stars in the photon energy range 0.1 ~ 2.4keV. Using the EXSAS software, three different coronal models have been considered to fit the PSPC data.

Model 1. An isothermal plasma with intervening absorption and three adjustable parameters - the gas temperature  $T$ , the

**Table 1.** Basic data of sample Stars

No.	stars	spectral type	$B - V$	magnetic strength (kG)	fill factor	reference	distance (pc)	category
1	HD166	K0V	0.75	2.1	0.34	1	15	S
2	HD1835	G2V	0.66	1.4	0.32	2	20	S
3	HD10476	K1V	0.84	1.0	0.17	2	8.4	R
4	HD17433	G9e	0.96	2.0	0.60	2	21	R
5	HD17925	K2V	0.87	1.5	0.35	2	8.3	S
6	HD20630	G5V	0.68	1.5	0.35	2	9.3	R
7	HD22049	K2V	0.88	1.0	0.30	2	3.3	R
8	HD22468	G9V	0.92	1.0	0.14	1	31	R
9	HD36395	M1.5V	1.47	1.5	0.15	2	5.9	R
10	HD39587	G0V	0.59	1.0	0.60	2	9.6	R
11	HD45088A	K2V	0.94	2.4	0.50	2	12	R
12	HD62044	K1III	1.12	1.1	0.70	3	56	R
13	HD101501	G8V	0.72	0.91	0.75	1	8.4	S
14	HD115404	K2V	0.93	2.1	0.20	1	12	B
15	HD118100	K5Ve	1.17	2.5	0.80	1	16	S
16	HD128620	G2V	0.88				1.3	S
17	HD131156	G8V	0.76	1.6	0.22	1	6.8	R
18	HD131511	K0V	0.83	1.0	0.52	2	12	B
19	HD131977	K4V	1.11	1.0	0.66	2	5.8	R
20	HD152391	G8V	0.76	1.7	0.18	1	15.9	S
21	HD152751	M3	1.57	$fB \simeq 1.0$		2	6.4	R
22	HD165341	K1V	0.86	1.2	0.17	1	5.0	B
23	HD185144	K0V	0.77	1.16	0.32	1	5.6	S
24	HD201091	K5V	1.18	1.2	0.24	2	3.4	R
25	HD209100	K4 - 5V	1.09	1.8 - 3.4	0.13	3	3	S
26	HD222107	G8III - IV	1.10	0.6	0.20	1	20	R
27	HD224085	K2V	1.01	3.0	0.6	4	17	dR
28	HD224677	M0Ve	1.19	2.8	0.60	1	16	B
29	HD283750	dK5ep	1.12	2.6	0.50	2	16.4	R
30	ADLeo	M4.5Ve	1.54	3.8	0.73	2	36	R

Col.(7) references are as follows: 1: Marcy 1984. 2: Saar 1990. 3: Mathys and Solansky 1989. 4: Saar 1996.

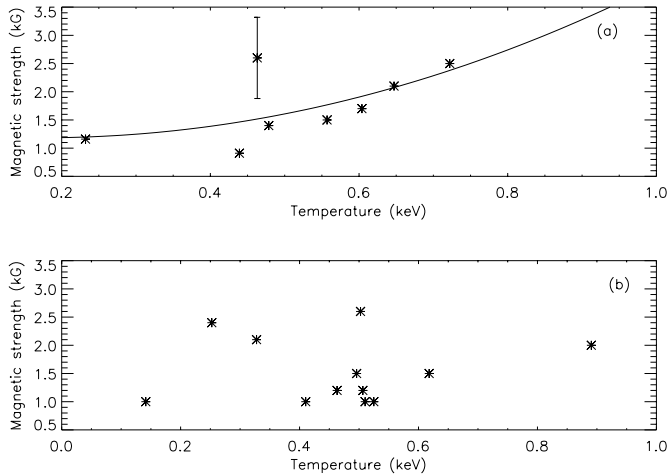


**Fig. 1a and b.** The one-temperature fit of the coronal temperatures vs. the magnetic field strength. **a** for single stars, the solid line is the best fit line. **b** for binaries and RS CVns.

emission measure  $EM$  at the given temperature and the hydrogen column density  $N_H$ . The defaults Raymand-Smith full-code model is used in this model.

Model 2. A plasma consisting of two isothermal components with four adjustable parameters,  $T_1$ ,  $EM_1$ ,  $T_2$  and  $EM_2$ . The Raymand-Smith fast mode model is used.

Model 3. A plasma consisting of two isothermal components with intervening absorption and five adjustable parameters,  $T_1$ ,  $EM_1$ ,  $T_2$ ,  $EM_2$  and  $N_H$ . We use the Raymand-Smith fast mode model.

### 3. Results

As single and binary stars exhibit markedly different behavior (Schachter et al. 1996), we divided the program stars into two subsamples, giving separate figures for the results for each subsample. Our approach to this analysis begins with the simplest model.

#### 3.1. One-temperature model

In Table 2 we present the one-temperature fit for all program stars which yield  $\chi_{ref}^2$  (column [8]) less than 3.5. columns (1) and (2) give sequence number and star name respectively. The

**Table 2.** Fitting parameters for one-Temperature model

No.	stars	$EM$ ( $10^{52}cm^{-3}$ )	$T$ (keV)	$\Delta T$ ( $10^{-2}keV$ )	$N_H$ ( $10^{19}cm^{-2}$ )	$\chi_{ref}$ number	$\chi^2$
1	HD166	6.008	0.6471	2.0	13.31	86	2.031
2	HD1835	7.683	0.4786	1.2	18.69	92	2.280
3	HD10476	0.103	0.1414	1.5	2.272	10	0.424
4	HD17433	59.38	0.8906	8.6	10.67	130	1.324
5	HD17925	2.118	0.5570	1.2	9.632	118	3.171
6	HD20630	1.525	0.6179	9.5	49.70	49	2.760
7	HD22049	0.383	0.5102	4.8	41.30	92	3.388
8	HD36395	0.114	0.4959	10.7	5.310	45	1.543
9	HD45088A	135.5	0.2524	10.8	486.9	94	2.476
10	HD101501	0.885	0.4391	2.3	9.090	42	1.463
11	HD115404	1.210	0.3277	2.2	25.09	13	0.941
12	HD118100	5.255	0.7220	1.6	9.207	135	1.629
13	HD128620	0.209	0.2423	0.3	0.001	60	2.402
14	HD131511	1.016	0.4103	1.8	7.800	98	2.807
15	HD131977	0.162	0.5249	8.9	1.140	60	1.615
16	HD152391	1.025	0.6039	3.9	6.366	24	1.472
17	HD165341	0.474	0.5064	3.3	34.09	7	2.858
18	HD185144	0.283	0.2321	1.3	8.320	13	1.441
19	HD201091	0.010	1.5130	33	3.090	23	1.897
20	HD209100	0.021	0.4631	1.8	3.540	29	1.557
21	HD283750	25.83	0.5025	4.3	22.50	119	3.126

**Table 3.** Fitting parameters for two-Temperature model

No.	stars	$EM_1$ ( $10^{50}cm^{-3}$ )	$T_1$ (keV)	$\Delta T_1$ ( $10^{-3}keV$ )	$EM_2$ ( $10^{50}cm^{-3}$ )	$T_2$ (keV)	$\Delta T_2$ ( $10^{-2}keV$ )	$\chi_{ref}$ number	$\chi^2$
1	HD166	17.797	0.1462	0.1	21.887	0.820	2.4	50	1.137
2	HD1835	15.095	0.1620	0.6	18.144	0.637	2.8	91	1.015
3	HD10476	0.322	0.1056	5.1	0.014	0.303	8.8	10	0.399
4	HD17433	224.3	0.2032	0.2	566.8	1.183	2.2	131	1.560
5	HD17925	6.391	0.1376	0.4	8.378	0.681	2.9	76	1.075
6	HD20630	1.638	0.6165	27	5.412	0.932	4.6	50	1.052
7	HD22049	0.662	0.3289	2.9	0.840	0.853	4.6	93	1.211
8	HD22468	1125	0.2181	0.1	4322	1.314	0.5	74	1.496
9	HD36395	0.913	0.2046	0.1	0.294	1.083	9.8	46	1.202
10	HD39587	0.546	0.4851	20	9.299	0.840	2.8	04	1.574
11	HD45088A	2.602	0.8622	8.5	13.32	0.902	1.8	96	1.603
12	HD62044	2444	0.2531	0.5	10511	1.260	0.8	01	1.982
13	HD101501	3.226	0.1454	0.1	2.161	0.629	7.9	22	0.887
14	HD115404	1.472	0.1568	1.1	1.386	0.588	18.7	12	1.001
15	HD118100	25.78	0.2029	0.9	37.855	1.159	1.3	87	1.029
16	HD128620	1.117	0.0981	0.3	0.198	0.392	1.2	60	1.183
17	HD131156	7.636	0.1785	1.0	5.168	0.843	1.7	40	1.426
18	HD131511	4.259	0.1563	0.0	1.969	0.743	6.5	99	1.242
19	HD131977	1.337	0.1686	0.5	0.601	0.976	6.1	61	1.329
20	HD152391	6.931	0.1562	0.0	4.227	0.666	11.2	13	0.935
21	HD152751	22.92	0.1999	0.5	19.159	1.057	0.9	70	1.224
22	HD165341	0.207	0.1523	2.3	1.504	0.730	8.6	7	0.573
23	HD185144	0.219	0.0680	0.5	0.851	0.162	0.7	13	1.529
24	HD201091	0.058	0.1913	2.7	0.104	0.918	7.8	22	1.122
25	HD209100	1.330	0.1770	0.9	0.468	0.967	5.2	49	1.101
26	HD224085	287.9	0.2353	0.8	1135.1	1.597	1.5	73	1.338
27	HD234677	98.20	0.2616	0.2	85.060	1.199	0.8	39	1.164
28	HD283750	80.64	0.2363	0.4	63.947	0.917	2.8	20	1.063
29	ADLeo	394.5	0.2012	0.2	500.86	1.063	0.5	92	1.785

**Table 4.** Fitting parameters for two-Temperature model with Intervening Absorption

<i>No. stars</i>	$EM_1$ ( $10^{50} \text{cm}^{-3}$ )	$T_1$ (keV)	$\Delta T_1$ ( $10^{-3} \text{keV}$ )	$EM_2$ ( $10^{50} \text{cm}^{-3}$ )	$T_2$ (keV)	$\Delta T_2$ ( $10^{-2} \text{keV}$ )	$N_H$ ( $10^{18} \text{cm}^{-2}$ )	$\chi_{ref}$ number	$\chi^2$	
1	HD166	17.67	0.145	5.1	21.89	0.818	2.4	0.01	50	1.139
2	HD1835	20.10	0.142	4.2	18.05	0.606	3.8	14.27	51	0.904
3	HD10476	0.322	0.105	2.5	0.014	0.302	2.3	0.01	10	0.399
4	HD17433	503.0	0.143	6.7	634.0	1.176	2.1	151.40	131	1.293
5	HD17925	7.351	0.128	4.1	8.306	0.678	2.5	18.75	117	0.890
6	HD20630	0.736	0.321	21	6.782	0.902	4.2	18.39	50	1.033
7	HD22049	0.638	0.323	37	0.963	0.890	4.1	0.01	93	1.129
8	HD22468	1243	0.214	1.3	4295	1.315	0.5	6.51	174	1.293
9	HD36395	0.913	0.204	7.4	0.294	1.082	9.9	0.01	46	1.203
10	HD39587	0.696	0.473	16	9.299	0.840	2.8	0.01	105	1.560
11	HD45088A	2.067	0.541	48	25.43	1.110	6.4	96.36	95	1.093
12	HD62044	2380	0.194	2.3	10461	1.199	0.4	21.06	201	1.798
13	HD101501	3.702	0.162	6.5	1.945	0.608	8.5	0.01	22	0.886
14	HD115404	4.469	0.147	23	1.259	0.741	18.7	152.30	13	0.612
15	HD118100	27.95	0.202	2.7	37.36	1.161	1.5	7.32	87	1.005
16	HD128620	1.119	0.098	1.3	0.197	0.393	1.3	0.04	60	1.184
17	HD131156	8.101	0.185	5.8	5.122	0.873	0.9	0.01	141	1.580
18	HD131511	4.404	0.094	1.2	1.960	0.767	6.1	0.01	99	1.250
19	HD131977	1.386	0.175	5.3	0.633	1.027	5.5	0.01	61	1.407
20	HD152391	7.235	0.161	8.1	4.091	0.692	13.4	0.01	13	0.948
21	HD152751	23.11	0.200	1.6	19.13	1.058	0.9	0.83	170	1.224
22	HD165341	1.299	0.129	28	9.923	0.788	6.3	178.80	7	0.118
23	HD185144	0.218	0.065	10	0.857	0.161	0.7	0.47	13	1.531
24	HD201091	0.058	0.191	23	0.104	0.918	7.8	0.01	22	1.122
25	HD209100	1.363	0.179	5.2	0.461	0.980	7.6	0.01	49	1.112
26	HD224085	286.1	0.235	1.8	1146	1.604	1.4	0.60	173	1.337
27	HD234677	101.2	0.266	1.9	82.48	1.213	0.9	0.01	139	1.220
28	HD283750	80.64	0.237	18	63.95	0.919	5.8	0.01	119	1.072
29	ADLeo	412.5	0.201	1.3	545.0	1.074	0.5	3.85	192	1.716

emission measures are given in column (3). The best fit temperature and its confidence intervals are given in columns (4) and (5). The column densities derived from the fits are given in column (6). Note that for most stars a statistically significant improvement of the fit was obtained by including finite values for  $N_H$ ; HD 128620 was the only program star for which no absorbing column was required.

Combining the resulting temperature  $T$  above with the magnetic field strength  $B$  given in Table 1, we plot the resulting X-ray temperature versus magnetic field strength: in Fig. 1a for the single stars, and **b** for the binary and RS CVn stars. From Fig. 1a, we see a correlation between the coronal temperatures and the magnetic field strength for single stars. This result suggests that the corona is heated magnetically. The best quadratic-polynomial fit is for  $B = (1.30 \pm 0.13) - (1.38 \pm 0.57)T + (3.97 \pm 0.59)T^2$ , with a reduced  $\chi^2$  of 1.62. But there is no correlation for the binary stars and RS CVn stars. This can be explained as follows: firstly, all of the companion stars contribute a considerable emission to the total observed luminosity as independent components, secondly in the close systems the orbital motion may induce fast surface rotational velocities by means of tidal coupling, and hence increase the

nonthermal heating of the individual stellar chromospheres and coronae (Maggio et al. 1990).

### 3.2. Two temperature model

Because the one-temperature model fails to fit some program stars, we use the two-temperature model to fit all sample stars. The fitting results which yield  $\chi_{ref}^2$  (column [10])  $< 2.5$  are shown in Table 3. Columns (1)-(5) in Table 3 are the same as the first five columns of Table 2 (presenting parameters for the low-temperature component of the model), while columns (6)-(8) provide analogous information for the high-temperature component.

In Fig. 2, we show - for acceptable two-temperature fits- the resulting X-ray temperature versus the magnetic field strength. From Fig. 2a, we see a remarkable correlation between the high-temperature component and the magnetic field strength for single stars, and the best quadratic-polynomial fit is  $B = (1.09 \pm 0.05) - (0.44 \pm 0.14)T + (1.64 \pm 0.10)T^2$ , with a reduced  $\chi^2 = 1.48$ . Also the best quadratic-polynomial fit for low-temperature components is  $B = (1.09 \pm 0.10) - (17.8 \pm 01.6)T + (107.4 \pm 5.9)T^2$ , with a reduced  $\chi^2 = 2.58$ . This value is too large to be acceptable. So we suggest that there

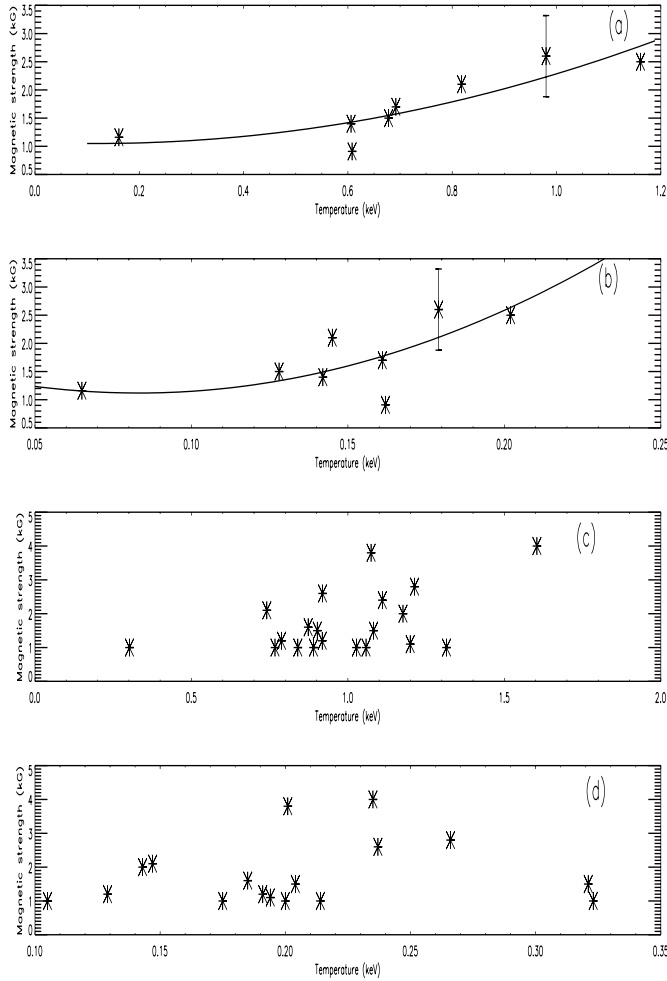


**Fig. 2a–d.** The two-temperature fit of the coronal temperatures vs. the magnetic field strength. **a** the high-temperature component for single stars, the solid line is the best fit line. **b** the low-temperature component for single stars. **c** the high-temperature component for binaries and RS CVns. **d** the low-temperature component for binaries and RS CVns.

is no correlation for the low-temperature component of single stars, which agrees with the result that the corona in quiet regions is heated accoustically while the corona in active regions is heated magnetically (Mullan & Fleming 1996). And there is no correlation either for the high-temperature component or for the low-temperature component of binaries and RS CVns.

### 3.3. Two temperature model with intervening absorption

In order to study the influence of intervening absorption, we use the two-temperature model with intervening absorption to fit all sample stars which yields  $\chi_{red}^2$  (column. [11])  $< 2.5$ . The results are shown in Table 4. Comparing with the Table 3, we find that, in most cases, the improvement is small when accounting for  $N_H$  values, but for some sample stars (HD62044, HD115404 and HD165341), a significant improvement in the fit is obtained when finite values of  $N_H$  are included. From Table 4, we see the high-temperature component for most of the single stars is lower than  $1keV$ , while for most of the binary and RS CVn

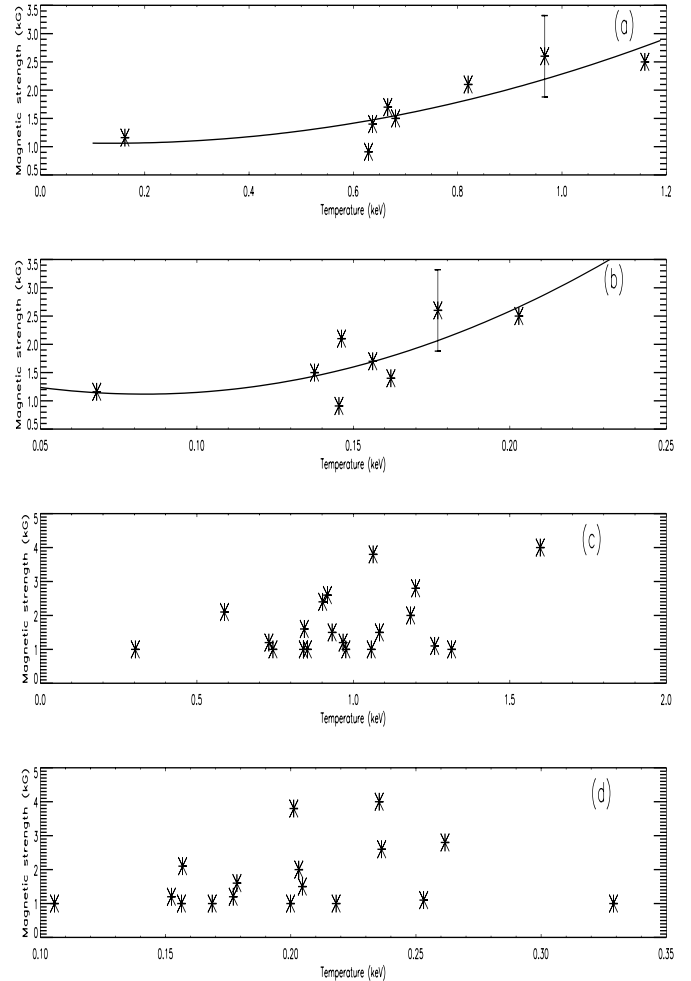


**Fig. 3a–d.** The two-temperature with intervening absorption fits of the coronal temperatures vs. the magnetic field strength. **a** the high-temperature component for single stars, the solid line is the best fit line. **b** the low-temperature component for single stars. **c** the high-temperature component for binaries and RS CVns. **d** the low-temperature component for binaries and RS CVns.

stars it is higher than  $1keV$ . Only star HD222107 fails to fit any coronal model.

We plot the resulting X-ray temperature versus magnetic field strength in Fig. 3, and we can gain the same results as for model 2 from Fig. 3. The best quadratic-polynomial fit for high-temperature component is  $B = (1.1 \pm 0.05) - (0.38 \pm 0.14)T + (1.6 \pm 0.10)T^2$ , with a reduced  $\chi^2 = 1.31$ , and  $B = (1.9 \pm 0.1) - (17.9 \pm 1.6)T + (107.4 \pm 5.9)T^2$ , with a reduced  $\chi^2 = 2.60$  for low-temperature component.

## 4. Conclusions

The correlation between the coronal temperatures and the photospheric magnetic field strength has been investigated. Some primary conclusions can be presented here: 1) There is a correlation between the high-temperature component and the magnetic field strength for single stars, which suggest that the high-temperature component is heated by the magnetic field. From

this result, we can estimate the magnetic field strength for single stars from the X-ray spectrum. We hope the future observed magnetic field can be compared with our estimation. 2) There is no correlation for the low-temperature component for single stars, the reason is that the low-temperature component is heated acoustically. 3) There is no correlation for binaries and RS CVns. 4) The best fit is the two-temperature model with intervening absorption.

*Acknowledgements.* This research was supported by the National Natural Science Foundation of China. We are very grateful to Prof. Xue-fu Liu for valuable comments on the magnetic fields for late-type stars and many stimulating discussions.

## References

- Falconer D.A., Moore R.L., Gray G.A. Shimizu T. 1997, ApJ 482, 519  
Maggio A., Vaiana G.S., Haisch B.M., et al. 1990, ApJ 348, 253  
Marcy G.W. 1984, ApJ 276, 286  
Mathys G., Solansky S.K. 1989, A&A 208, 189  
Mullan D.J. Fleming T.A. 1996, ApJ 464, 890  
Saar S.H. 1990, in IAU Symp. 138, Solar Photosphere: Structure, Convection, and Magnetic Fields, ed. J.O. Stenflo (Dordrecht: Kluwer), 427  
Saar S.H. 1996, in IAU Symp. 176, Stellar Surface Structure, ed. K.G. Strassmeier and J.L. Linsky, 237  
Schachter J.F., Remillard R., Saar S. H. et al. 1996, ApJ 463, 747  
Schmitt J.H.M.M. 1994, ApJS 90, 734